A&A 398, 583–587 (2003)
DOI: 10.1051/0004-6361:20021563

Astronomy & Astrophysics

Centimeter wavelength continuum observations of young stellar objects in the dark cloud DC 303.8–14.2

K. Lehtinen[1] and J. L. Higdon[2,3]

[1] Observatory, Tähtitorninmäki, PO Box 14, 00014, University of Helsinki, Finland
[2] Kapteyn Astronomical Institute, PO Box 800, 9700 AV Groningen, The Netherlands
[3] Australia Telescope, Paul Wild Observatory, Locked Bag 194, Narrabri, NSW, Australia

Received 27 May 2002 / Accepted 28 October 2002

Abstract. We have made radio continuum observations with the ATCA (Australia Telescope Compact Array)⋆ at 3 and 6 cm of the dark cloud DC 303.8–14.2 in order to study the content of young stellar objects (YSOs) in this cloud. Four unresolved sources were found within the cloud's boundary. One of these in coincident with IRAS 13036–7644, a very low luminosity YSO driving a bipolar molecular outflow. We have interpreted its emission in terms of optically thin thermal free-free emission, although within errors also non-thermal emission is possible. The possible source of ionization is discussed.

Key words. stars: formation – ISM: individual objects: DC 303.8–14.2 – ISM: individual objects: IRAS 13036–7644 – ISM: clouds – radio continuum: ISM

1. Introduction

The globule DC 303.8–14.2 (Hartley et al. 1986) is located in the eastern part of the Chamaeleon II dark cloud complex. It harbours the IRAS point source IRAS 13036–7644, which possesses a spectral energy distribution (SED) typical for a young stellar object (YSO); the flux densities at 12, 25, 60 and 100 μm are 0.10, 1.08, 6.28 and 22.01 Jy, respectively (Prusti et al. 1992). Its coordinates are $\alpha(1950) = 13^{\rm h}3^{\rm m}41.4^{\rm s}$, $\delta(1950) = -76°44'3''$, and the positional error ellipse has semi minor and major axes of $6''$ and $20''$.

In their continuum survey at 1.3 mm Henning et al. (1993) measured a flux density of 223 ± 49 mJy for this object. This emission is most probably thermal emission from cold circumstellar dust grains.

Lehtinen (1997) has observed DC 303.8–14.2 at millimeter molecular lines, and found that the high density tracers CS($J = 2$–1), CS($J = 3$–2) and $H_2CO(2_{12}$–$1_{11})$ show asymmetrical douple-peaked profiles that are typical for a collapsing cloud. IRAS 13036–7644 is located at the center of a bipolar molecular outflow; thus it is probably the driving source of this outflow (Lehtinen 1997), although it is possible that another, even younger source could be driving the outflow. In addition, there seems to be another red-shifted outflow component at $(\Delta\alpha, \Delta\delta) \approx (-4', -2')$, and possibly a blue-shifted outflow component located to the west from it (see Fig. 1).

Chen et al. (1997) have calculated bolometric luminosities and temperatures (as defined in Myers & Ladd 1993) for YSOs in nearby molecular clouds. They find values of 0.47 $L_\odot$ and 63 K for IRAS 13036–7644. In a bolometric luminosity-temperature diagram of Chen et al. (1995) IRAS 13036–7644 is located near the division line between Class 0 and Class I sources. However, in the absence of flux measurements between 100 μm and 1.3 mm it is not possible to deduce reliably the class of the IRAS source.

It is known that even very low luminosity sources associated with bipolar outflows produce radio continuum emission. In the context of Bok globules, Yun et al. (1996) have searched for radio continuum emission from globules using the VLA at 3.6 cm, and found that most of the globules that have a radio continuum source within their optical extent, have been previously found to have an associated molecular outflow. This relationship between continuum radiation and outflows led Yun et al. (1996) to suggest that the continuum radiation is coming from circumstellar gas which is shock-ionized by the stellar wind from the YSO. This stellar wind is also the power source of the molecular outflow.

The youngest stellar objects known so far (possibly true protostars, so called Class 0 objects) are so deeply embedded in their parent cloud that they are detectable only at mid-infrared and at longer wavelengths. Sometimes these objects can be detected only due to the associated molecular outflow, and by means of their cm-wavelength continuum radiation. Most of the objects that have been classified as Class 0 objects have also been detected in centimeter wavelength continuum radiation (Yun et al. 1996).

The main motivation of this study was to detect cm-wavelength continuum radiation from the IRAS 13036–7644.

Send offprint requests to: K. Lehtinen,
e-mail: kimmo.lehtinen@helsinki.fi

Radio flux measurements would complement the existing SED, and permit the determination of a more accurate luminosity. The spectral index, α (defined to be $S_\nu \propto \nu^\alpha$), of the emission between 3 and 6 cm can be used to distinguish between the various emission mechanisms. Our observations could also reveal new YSOs that are so heavily embebbed that they are not detected by IRAS, i.e. possible Class 0 objects.

2. The origin of radio continuum emission from YSOs

In general, the radio continuum sources associated with YSOs are weak, and they are unresolved except with a subarcsecond resolution. It has been found that the shape of the SED at cm-wavelengths for YSOs is characteristic of thermal free-free emission. However, it is also known that this emission can not arise from a compact H II region which is ionized by stellar photons from the YSO. The required ionizing photon flux is that of an early B type star (Torrelles et al. 1985), which is orders of magnitude greater than the expected flux from the associated YSOs. Thus, there must be other mechanisms involved which contribute to the inferred ionization, unless YSOs produce much more Lyman continuum radiation than expected.

The different mechanisms can be distinguished by the shape of the radio spectrum, if observations over a large enough wavelength range are available. In the following we discuss some of them briefly. For a review of ionized winds from young stellar objects see André (1987) and Panagia (1991).

2.1. Thermal emission from accretion

The accretion models are of special interest in this case, because there is evidence of mass infall towards the IRAS source, based on millimeter molecular line observations (Lehtinen 1997).

In Bertout's (1983) model of accretion onto a protostellar core the radio-emitting region is photoionized by soft X-ray and EUV radiation from an accretion shock around a protostellar core. In this model the spectrum has roughly a $S_\nu \propto \nu^{0.6}$ shape.

Felli et al. (1982) have modelled thermal emission from an extended, ionized circumstellar envelope which is in a state of accretion. This model produces a non-power-law flat spectrum, $S_\nu \propto \nu^{-0.1} - \nu^{0.1}$ (Felli et al. 1982; Panagia 1991; André 1987). The predicted flux density is (Panagia 1988)

$$S_\nu(\mathrm{acc}) \approx 8.18 \left(\frac{\nu}{10\,\mathrm{GHz}}\right)^{-0.1} \left(\frac{T}{10^4\,\mathrm{K}}\right)^{-0.35} \times \left(\frac{M}{M_\odot}\right)^{-1} \left(\frac{\dot{M}_\mathrm{accr}}{10^{-7}\,M_\odot\,\mathrm{yr}^{-1}}\right) \left(\frac{d}{\mathrm{kpc}}\right)^{-2} \ln\left(\frac{r_\infty}{r_\mathrm{c}}\right) \mathrm{mJy} \quad (1)$$

where $\dot{M}_\mathrm{accr}$ is the mass accretion rate, M and d are the stellar mass and distance, T is temperature, r_c is the radius at which the optical depth equals 3/4, and r_∞ is the outer boundary (generally the accretion radius). This equation is valid when $r_\infty \gg r_\mathrm{c}$.

2.2. Thermal ionized stellar wind

Ionized stellar wind models have been presented which are either spherically symmetric (Panagia & Felli 1975; Wright & Barlow 1975; Felli et al. 1982; Panagia 1991) or nonsymmetric (Schmid-Burgk 1982; Reynolds 1986). In the case of ionized stellar wind in general, the frequency dependence has a large range from $S_\nu \propto \nu^{-0.1}$ to $S_\nu \propto \nu^2$ (Reynolds 1986 and references therein). In the case of a spherical, fully ionized, isothermal and constant-velocity flow, which is considered as the "standard" spherical wind, the 3 to 6 cm spectral index is 0.6 for large opacity. Significant deviations from the spectral index or flux predicted by the "standard" spherical wind occur only if the solid angle filled by the flow varies systematically with radius or the wind is highly anisotropic (Schmid-Burgk 1982; Reynolds 1986).

2.3. Thermal shock emission

Shock-induced ionized model was first proposed by Torrelles et al. (1985). The required ionizing photons are produced when a powerful, high velocity neutral stellar wind is shocked by dense matter surrounding the YSO. The now collimated wind produces a molecular outflow. The shock-ionization model predicts a $S_\nu \propto \nu^{-0.1}$ dependence for radio continuum emission (Curiel et al. 1987, 1989) The predicted flux density in the optically thin case is (Curiel et al. 1989)

$$S_\nu(\mathrm{shock}) \approx 3.98 \times 10^{-2} \left(\frac{\nu}{5\,\mathrm{GHz}}\right)^{-0.1} \left(\frac{T}{10^4\,\mathrm{K}}\right)^{0.45} \times \left(\frac{\dot{M}}{10^{-7}\,M_\odot\,\mathrm{yr}^{-1}}\right) \left(\frac{v_\infty}{100\,\mathrm{km\,s}^{-1}}\right)^{0.68} \left(\frac{d}{\mathrm{kpc}}\right)^{-2} \times \left(\frac{\Omega}{4\pi}\right) \mathrm{mJy} \quad (2)$$

where $\dot{M}$ is the mass loss rate, v_∞ is the terminal velocity of the wind, and $\frac{\Omega}{4\pi}$ is the solid angle subtended by the surrounding matter as seen from the star.

2.4. Thermal dust emission

Yet another possible source of emission is thermal emission from dust grains, which has a positive spectral index. If we assume a ν^4 frequency dependence for emission between 1.3 mm and 3 cm, typical for optically thin dust emission, the 223 mJy flux at 1.3 mm (Henning et al. 1993) can be used to predict a flux density of 0.4 μJy at 3 cm for the IRAS 13036–7644.

2.5. Non-thermal emission

A source that has a non-thermal spectrum ($\alpha < -0.1$) would probably be a nonstellar background object. However, not every source with $\alpha < -0.1$ is necessarily a nonstellar object; Abbot et al. (1984) have detected non-thermal emission from two O stars. For YSOs the relevant non-thermal emission process is synchrotron radiation.

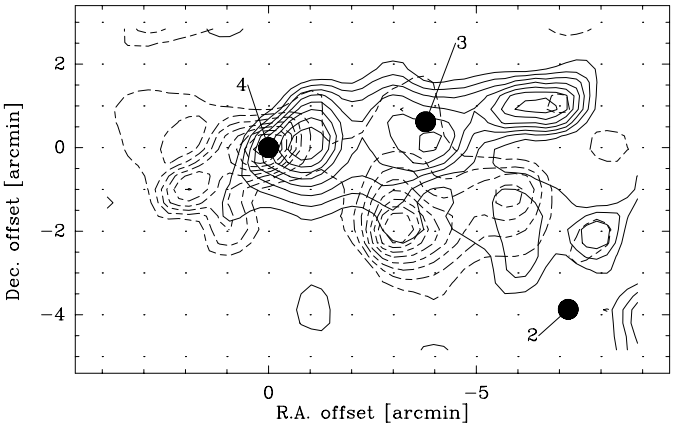

Fig. 1. A map of the integrated intensity of ^{12}CO (J = 1–0) emission over the velocity intervals 0–1 (solid contours) and 6–7 km s^{-1} (dashed contours). The contours are from 0.1 to 0.8 in steps of 0.1 K km s^{-1}. The radio continuum sources are indicated with filled circles, with numbers referring to the list in Table 1. We identify source #4 with IRAS 13036–7644. Source #1 is located outside this map. The (0,0) position is at RA(1950) = $13^{\rm h}3^{\rm m}41\overset{\rm s}{.}4$, Dec.(1950) = $-76°44'18\overset{''}{.}0$.

3. Observations

We imaged two fields in DC 303.8–14.2 at 3.5 and 6.3 cm wavelengths with the ATCA during 13–14 March 1997. The array was in the 1.5D configuration, which gave a range of interferometer spacings between 102 m and 4.4 km, and the correlator was set to provide a total bandpass of 128 MHz at both 3 and 6 cm. The primary beam *FWHM* at 6 cm and 3 cm are 10′ and 5′, respectively. The first field was centered on IRAS 13036–7644, while the second was offset 5′ West and 2′ South from this position. Five minute integrations in each field were alternated with short scans of a nearby secondary calibrator throughout the 14-hour observing period. All fluxes were tied to the standard source 1934-638 (S(6 cm) = 4.81 Jy, Reynolds 1994). The absolute flux calibration accuracy is expected to be 10%. Reference pointing was used throughout to minimize positional uncertainty. Data editing, calibration, and mapping was done using NRAO's AIPS software package. Naturally weighted maps were made for both fields and frequencies. These had rms map noises after CLEANing of 50 μJy/beam (3 cm) and 48 μJy/beam (6 cm), which are both near the expected values. The synthesized beams have *FWHM* of $3.6'' \times 2.8''$ (3 cm) and $5.1'' \times 4.5''$ (6 cm). Finally, each map was corrected for primary beam attenuation.

4. Results and discussion

We detected seven sources in all, but only four within DC 303.8–14.2's boundaries. Of these, two were detected at both 3 and 6 cm. All the sources were unresolved, and no large scale structure was apparent in the maps. We therefore used the AIPS task IMFIT to derive fluxes and positions, along with their uncertainties, by fitting 2-dimensional Gaussians to each source. We have verified the unresolved nature of the sources by making contour plots of the sources along with the plots of the beams. The measured positions, deconvolved angular sizes, integrated fluxes and derived 3 cm–6 cm spectral indices are shown in Table 1. The errors of fluxes and spectral indices include only the statistical noise of the data, not the calibration uncertainty. Note that the source #1 is situated beyond the 3 cm primary beam, and is located in the outer parts of the optical extent of DC 303.8–14.2. When calculating flux upper-limits for sources #1 and #2, which were not detected at both wavelengths, we assumed a point source with a peak intensity twice times the map noise level.

The source #3 has a spectral index $\alpha = -0.7$, indicating non-thermal spectrum. Interestingly, it is located exactly on the axis of the blue-shifted outflow component, and raises the question whether it is related to the outflow, because non-thermal emission from Herbig-Haro objects has been detected (Reipurth 1991). In this context, however, we do not consider this source any longer.

Source #2 is detected only at 3 cm. Using a 2σ value for the flux at 6 cm, its spectral index is $\alpha > 1.1$, i.e. the emission is thermal, possibly from a source located within the cloud.

4.1. Emission diagnostics for the IRAS source

Source #4 is located within the positional error ellipsoid of IRAS 13036–7644, thus we have identified these sources to be the same. The observed flux is typical for YSOs located in Bok globules (Yun et al. 1996). The spectral index α of this source is -0.4 ± 0.1, which indicates non-thermal emission, but is close to the value of α for optically thin thermal emission, -0.1. A calibration error of 10% at both wavelengths is enough to bring the spectral index into the regime of optically thin thermal emission. We note that if we simply take the peak value of the observed surface brightness, which for point sources is the same as the total flux, we derive a spectral index of -0.1. We conclude that within uncertainties, the spectral index of the source #4 is consistent with optically thin thermal emission.

In the case that a source is resolved, the most secure way to discriminate between thermal and non-thermal emission would be the brightness temperature: thermal emission is charecterized by low brightness temperature, $T_{\rm b} \leq 10^4$ K, while non-thermal emission is charecterized by high brightness temperature, $T_{\rm b} \geq 10^{7.5}$ K. However, none of the measured *FWHM* for our sources are sufficiently larger than the synthesized beams to qualify as being resolved.

The value of α rules out the Bertout's (1983) accretion model, and the "standard" spherical wind model, which both have $\alpha \approx 0.6$. We do not consider in detail the nonspherical stellar wind models (Schmid-Burgk 1982; Reynolds 1986) due to complexities of these models compared with our sparse data. We just note that for a fully ionized collimated flow, in the case of constant temperature, velocity and ionization fraction, i.e. the "standard" case except that the flow is confined, the spectral index has the form

$$\alpha = 1.3 - 0.7/\epsilon \tag{3}$$

where ϵ is the power-law index which determines the dependence of the width of the flow (w) on the distance from the central object (r), $w \propto r^{\epsilon}$ (Reynolds 1986). If we use the value $\alpha = -0.1$, we derive $\epsilon = 0.5$.

Table 1. The radio continuum sources detected in DC 303.8–14.2. Flux upper-limits are calculated assuming a point source with a peak intensity of twice the map rms. Note that source #1 is located outside the 3 cm primary beam. The positional accuracy is expected to be better than 2″. Source #4 is coincident with IRAS 13036–7644. The deconvolved angular size is the measured *FWHM* along the major and minor axes at 6 cm (or at 3 cm if 6 cm data not available) with uncertainty in parentheses. All the sources are unresolved. The quantity S is the intensity integrated over the source. The errors of S and α include only the noise of the data, not the calibration uncertainty.

Source number	Position α(1950)	δ(1950)	Angular size [″]	S(3 cm) [mJy]	S(6 cm) [mJy]	α
1	$13^h01^m01\overset{s}{.}79$	−76°40′10″.6	5.7 × 4.5 (0.7)	<0.48	3.22 ± 0.34	<−3.2
2	$13^h01^m36\overset{s}{.}58$	−76°47′57″.5	6.3 × 4.5 (0.9)	0.30 ± 0.13	<0.16	>1.1
3	$13^h02^m36\overset{s}{.}46$	−76°43′27″.2	5.0 × 3.1 (0.3)	1.00 ± 0.17	1.55 ± 0.15	−0.7 ± 0.1
4	$13^h03^m42\overset{s}{.}11$	−76°44′08″.7	5.3 × 4.2 (0.5)	0.92 ± 0.11	1.16 ± 0.11	−0.4 ± 0.1

In the following we discuss in more detail the models which predict a spectral index α compatible with our observations. A lower limit to the flux from accretion (Eq. (1)) can be predicted by setting the logarithmic term to unity. In reality we expect the condition $r_\infty \gg r_c$ to be prevalent, i.e. the logarithmic term is much greater than unity. Assuming that $T = 10^4$ K, $M = 1\,M_\odot$, and $d = 200$ pc, the mass accretion rate required to produce the observed flux is $\sim 4 \times 10^{-10}\,M_\odot\,\mathrm{yr}^{-1}$. This rate is about four to five orders of magnitudes smaller than the typical rate expected for low-mass YSOs, $\sim 10^{-6}$–$10^{-5}\,M_\odot\,\mathrm{yr}^{-1}$. Clearly, the flux predicted by this spherical, free-fall accretion model has to be reduced somehow, if it is to be the emission mechanism for a YSO with a typical mass accretion rate. The flux can be reduced if e.g. (1) the accretion is not spherical due to a disk and/or magnetic fields, as evidenced by observations in other systems and models, (2) the accretion is not described by free-fall motions due to e.g. magnetic fields, turbulence, outflow or winds.

The flux predicted by the shock emission model (Eq. (2)) has been calculated by assuming $T = 10^4$ K, $\dot{M}$ between 10^{-8}–$10^{-7}\,M_\odot\,\mathrm{yr}^{-1}$, $v_\infty = 200\,\mathrm{km\,s}^{-1}$, and $d = 200$ pc; $S_\nu(\mathrm{shock}) \approx (\Omega/4\,\pi)(0.2 - 2)$ mJy. Due to the many unknown parameters this estimate is only suggestive, but it shows that with typical parameters the shock emission model can produce the observed flux.

The predicted flux of thermal dust emission is about two orders of magnitudes less than the rms noise level in the maps. Furthermore the flatness of the spectrum between 3 and 6 cm is not consistent with thermal emission from dust. The 1.3 mm continuum emission around IRAS 13036–7644 is extended on a map made of 3×3 grid points with a grid distance of 20″, measured with the SEST (Swedish ESO Submillimeter Telescope) bolometer (Lehtinen et al. unpublished data). Thus thermal emission from dust grains at cm-wavelengths would also be extended. We can exclude the dust emission as mechanism for source #4.

5. Conclusions

We have conducted a search for radio continuum emission from young stellar objects in the globule DC 303.8–14.2 using the Australia Telescope Compact Array. We detected an unresolved source which is coincident positionally with the IRAS 13036–7644, a deeply embedded object driving a bipolar molecular outflow. Based solely on the spectral index, we can not make a firm distinction between non-thermal and optically thin thermal free-free emission.

None of the other sources has an associated IRAS point source. The source #3 is located on the ^{12}CO outflow component, and it has a non-thermal spectral index, $\alpha = -0.7$. For the source #2, also within the cloud, we can derive only a lower limit for the spectral index, $\alpha > 1.1$, which indicates thermal emission. Not much of its nature can be said at this point, but it is a good candidate for being a YSO, possibly a Class 0 protostar, within the cloud.

The origin of ionization in these low-luminosity objects has been studied on the basis of the observed fluxes at 3 and 6 cm. The spectral index and the observed fluxes of the IRAS source are consistent with models where the source of emission is circumstellar gas shocked and ionized by the stellar wind (Torrelles et al. 1985) or a mass accreting envelope (Felli et al. 1982). The accretion model of Felli et al. (1982), when applied with physical parameters typical for a low-mass YSO, produces much more flux than what is observed. Either the mass accretion is exceedingly low, or, more probably, the spherical, free-fall model is not applicable here. The shock-induced model has more unknown parameters, but it can produce a flux which is compatible with observations.

Our observations have added one more object to the list of continuum emission from low-luminosity embedded YSOs that are powering molecular outflows. In order to deduce the real source of emission, continuum observations at a wider spectral region are necessary. In addition, high angular resolution observations capable of resolving the structure of the sources would be most instructive.

Acknowledgements. We wish to thank the ATCA staff for operating the telescope during our observations. The work of K.L. has been supported by the Vilho, Yrjö and Kalle Väisälä foundation of the Finnish Academy of Science and Letters, and by the Finnish Academy through grant No. 1011055, which is gratefully acknowledged. We thank the referee for useful comments.

References

Abbot, D. C., Bieging, J. H., & Churchwell, E. 1984, ApJ, 280, 671
André, P. 1987, in Protostars and Planets, ed. T. Montmerle, & C. Bertout (Saclay: CEA/Doc)

Bertout, C. 1983, A&A, 126, L1
Chen, H., Myers, P. C., Ladd, E. F., & Wood, D. O. S. 1995, ApJ, 445, 377
Chen, H., Grenfell, T. G., Myers, P. C., & Hughes, J. D. 1997, ApJ, 478, 295
Curiel, S., Cantó, J., & Rodríguez, L. F. 1987, Rev. Mex. Astron. Astrofis., 14, 595
Curiel, S., Rodríguez, L. F., Cantó, J., et al. 1989, Ap. Lett. Comm., 27, 299
Felli, M., Gahm, G. F., Harten, R. H., Liseau, R., & Panagia, N. 1982, A&A, 107, 354
Hartley, M., Manchester, R. N., Smith, R. M., Tritton, S. B., & Goss, W. M. 1986, A&AS, 63, 27
Henning, Th., Pfau, W., Zinnecker, H., & Prusti, T. 1993, A&A, 276, 129
Lehtinen, K. 1997, A&A, 317, L5
Myers, P. C., & Ladd, E. F. 1993, ApJ, 413, L47
Panagia, N., & Felli, M. 1975, A&A, 39, 1
Panagia, N. 1988, in Galactic and extragalactic star formation, ed. R. E. Pudritz, & M. Fich (Dordrecht: Kluwer)
Panagia, N. 1991, in The physics of star formation and early stellar evolution, ed. C. J. Lada, & N. D. Kylafis (Kluwer Academic Publishers)
Prusti, T., Whittet, D. C. B., Assendorp, R., & Wesselius, P. R. 1992, A&A, 260, 151
Reipurth, B. 1991, in The physics of star formation and early stellar evolution, ed. C. J. Lada, & N. D. Kylafis (Kluwer Academic Publishers)
Reynolds, S. P. 1986, ApJ, 304, 713
Reynolds, J. 1994, ATNF Tech. Document Series 39.3/040
Schmid-Burgk, J. 1982, A&A, 108, 169
Torrelles, J. M., Ho, P. T. P., Rodríguez, L. F., & Cantó, J. 1985, ApJ, 288, 595
Wright, A. E., & Barlow, M. J. 1975, MNRAS, 170, 41
Yun, J. L., Moreira, M. C., Torrelles, J. M., Afonso, J. M., & Santos, N. C. 1996, ApJ, 111, 841